Annals of Botany **107**: 953–964, 2011
doi:10.1093/aob/mcr042, available online at www.aob.oxfordjournals.org

ANNALS OF BOTANY
Founded 1887

Anatomical features associated with water transport in imperforate tracheary elements of vessel-bearing angiosperms

Yuzou Sano[1,*], Hugh Morris[2,†], Hiroshi Shimada[1], Louis P. Ronse De Craene[3] and Steven Jansen[2,‡]

[1]*Graduate School of Agriculture, Hokkaido University, Sapporo 060-8589, Japan,* [2]*Jodrell Laboratory, Royal Botanic Gardens Kew, Richmond, Surrey TW9 3DS, UK and* [3]*Royal Botanic Garden Edinburgh, 20A Inverleith Row, Edinburgh EH3 5LR, Scotland, UK*

[†]*Present address: The Forestry and Arboriculture Department, Plumpton College, Ditchling Road, Plumpton, NR Lewes, East Sussex BN7 3AE, UK*

[‡]*Present address: Institute of Systematic Botany and Ecology, Ulm University, Albert-Einstein-Allee 11, D-89081 Ulm, Germany*

* *For correspondence. E-mail pirika@for.agr.hokudai.ac.jp*

Received: 22 October 2010 Returned for revision: 29 November 2010 Accepted: 26 January 2011 Published electronically: 8 March 2011

• *Background and Aims* Imperforate tracheary elements (ITEs) in wood of vessel-bearing angiosperms may or may not transport water. Despite the significance of hydraulic transport for defining ITE types, the combination of cell structure with water transport visualization *in planta* has received little attention. This study provides a quantitative analysis of structural features associated with the conductive vs. non-conductive nature of ITEs.
• *Methods* Visualization of water transport was studied in 15 angiosperm species by dye injection and cryo-scanning electron microscopy. Structural features of ITEs were examined using light and electron microscopy.
• *Key Results* ITEs connected to each other by pit pairs with complete pit membranes contributed to water transport, while cells showing pit membranes with perforations up to 2 μm were hydraulically not functional. A close relationship was found between pit diameter and pit density, with both characters significantly higher in conductive than in non-conductive cells. In species with both conductive and non-conductive ITEs, a larger diameter was characteristic of the conductive cells. Water transport showed no apparent relationship with the length of ITEs and vessel grouping.
• *Conclusions* The structure and density of pits between ITEs represent the main anatomical characters determining water transport. The pit membrane structure of ITEs provides a reliable, but practically challenging, criterion to determine their conductive status. It is suggested that the term tracheids should strictly be used for conductive ITEs, while fibre-tracheids and libriform fibres are non-conductive.

Key words: Cryo-SEM, dye injection, fibre-tracheid, libriform fibre, pit membrane, pit morphology, secondary xylem, imperforate tracheary element (ITE), tracheid, vessel, water transport.

INTRODUCTION

Imperforate tracheary elements (ITEs) are generally defined as unicellular tracheary cells that lack a perforation plate and are therefore only connected to each other by pit pairs, which represent openings in the secondary cell wall. Vessel elements, however, are connected to each other by openings or perforations in the primary and secondary cell wall, which is usually referred to as the end wall or perforation plate. Depending on the absence or presence of various degrees of pit membrane remnants associated with vessel perforations, the end wall openings are either complete or imperfect, making the distinction between a thin, porous pit membrane and a perforation plate not always clear (Butterfield, 1995; Carlquist, 2001, 2009*a*). Therefore, additional criteria for the definition of a perforation plate are: (*a*) at least an appreciable area of the end wall should be free from pit membrane remnants and (*b*) the end wall should be morphologically differentiated from the lateral vessel wall (Carlquist, 2009*a*). As vessel elements are generally much wider than ITEs and form multicellular vessels varying from a few millimetres to several metres in length, they represent major pathways for long-distance water transport in secondary xylem of vessel-bearing angiosperms (Tyree and Zimmermann, 2002). Although ITEs have been suggested to provide an additional hydraulic pathway, most xylem physiological studies on vessel-bearing angiosperms simply ignore the conductive nature of ITEs because they are not regarded as contributing to the water transport process to any significant extent (Tyree and Zimmermann, 2002; Sperry *et al.*, 2007; Hudson *et al.*, 2010, Pittermann, 2010). Moreover, the fact that only some types of ITEs transport water makes the hydraulic contribution of ITEs rather complicated (Braun, 1970; Ellmore and Ewers, 1985, 1986; Sano *et al.*, 2005; Umebayashi *et al.*, 2008, 2010).

The conductive or non-conductive nature of ITEs provides an important criterion for classifying these cells as fibre-tracheids, libriform fibres and tracheids (Carlquist, 2001). There is general consensus that tracheids with their characteristically distinct pit borders contribute to water transport, and that libriform fibres, which form the major mechanical cells in wood because of their mostly thick cell walls and narrow lumina, are not conductive (Metcalfe and Chalk, 1983). However, depending on the delimitation of tracheids and fibre-tracheids, some ITEs present a problem as these cells may

contribute to both water transport and mechanical support, representing a morphological continuum between conductive and non-conductive ITEs (Metcalfe and Chalk, 1983). Unfortunately, observations on the conductivity of ITEs in combination with detailed anatomical observations remain limited to fewer than a dozen species of angiosperms (Sano *et al.*, 2005). Because there has been no general consensus on the definitions of ITEs, controversy about how to distinguish between different cell types has been common for many years and probably will continue for years to come (Reinders, 1935, 1951; Bailey, 1936; Koek-Noorman, 1969; Baas, 1986; Carlquist, 1986*a*, *b*, 2001; Baas and Magendans, 1999; Magendans, 1999).

Conductivity of ITEs has mainly been suggested to be associated with the following characters: the diameter of the cell lumen, size of the pit border, pit density, distribution of pits on radial and/or tangential walls, circularity of the pit border, cell length, presence of septa (i.e. thin, unpitted, transverse walls) in the cell lumen, connectivity to other xylem cell types, and the inclusion of starch and mineral inclusions. The amount of water conducted through conduits is proportional to the fourth power of the conduit diameter if other conditions such as pressure gradient and temperature are identical according to Hagen-Poiseuille's law (Tyree and Zimmermann, 2002). Conductive ITEs typically show larger and more circular pit borders, and a higher pit density as compared with non-conductive cells (Carlquist, 2001). Also, conductive cells are suggested to be non-septate (Parameswaran and Liese, 1969; Butterfield and Meylan, 1976) and not to show cell inclusions. While various wood anatomical studies provide accurate information about the bordered pit size and length of tracheary elements (e.g. Jansen *et al.*, 2001; Lens *et al.*, 2008, 2009), few wood anatomical descriptions include information on the number of pits per ITE (Lens *et al.*, 2003). Recently, Sano and Jansen (2006) indicated that perforated pit membranes (i.e. pit membranes with a large opening that is much wider than the largest pit membrane pore) are commonly present between ITEs with minutely bordered pits, while sheet-like (non-perforated) pit membranes without perforations are consistently present between cells with distinctly bordered pits.

This report aims to provide detailed observations of the water transport capacity of ITEs in a selected number of vessel-bearing angiosperm shrubs and trees in order to test previously established hypotheses about anatomical characteristics of ITEs associated with water transport. The conductive potential of ITEs is determined by conducting dye injection experiments using living shrubs and small trees (Sano *et al.*, 2005). A central question is whether there is indeed a morphological continuum between conductive and non-conductive ITEs and how the conductive nature can be translated into various types of ITE definitions. Special attention is paid to the micromorphology of pits. It is hypothesized that perforated pit membranes occur in non-conductive ITEs, while conductive elements show intact pit membranes. Moreover, potential correlations between spatial vessel distribution and types of ITEs will be tested given the strong, but frequently overlooked correlations previously reported (Carlquist, 1966, 1984, 1987, 2001, 2009*b*; Rosell *et al.*, 2007).

MATERIALS AND METHODS

Plant material

Young shrubs or trees of 15 angiosperm species were selected. The site, size and age of species selected are shown in Table 1. The dye injection experiments at the Royal Botanic Gardens, Kew were carried out between late May and early June 2007. The experiments at Hokkaido University (Sapporo and Tomakomai, Hokkaido, Japan) were carried out between late June and early October 2003–2007. At both sites, the dye solutions were introduced on a sunny day during early afternoon.

Since the dye injection experiment was destructive, species selection was mainly limited to woody species that were common in Kew and Sapporo and for which permission was obtained to kill one specimen. In addition, selection was aimed to include species with different wood anatomical patterns, including both diffuse-porous and ring-porous species. One sample per species was studied.

TABLE 1. *List of species studied with reference to their abbreviation, origin (location), diameter at breast height (dbh) and age; one sample per species was examined*

Species	Abbreviation	Location	Height (m)	dbh (cm)	Age (years)
Acer pictum subsp. *mono*	*Am*	Sapporo	4·2	3·5	10
Acer pseudoplatanus	*Ap*	Kew	5·2	4	5
Betula japonica	*Bj*	Sapporo	7·5	5·5	9
Cercidiphyllum japonicum	*Cj*	Sapporo	5·4	4·5	9
Fagus crenata	*Fc*	Sapporo	5·9	5	11
Fraxinus mandshurica var. *japonica*	*Fm*	Sapporo	5·4	4	12
Ilex aquifolium	*Ia*	Kew	5·0	5	5
Juglans mandshurica var. *sieboldiana*	*Jm*	Sapporo	5·2	3	9
Kalopanax septemlobus	*Ks*	Sapporo	5·3	6	11
Prunus sargentii	*Ps*	Tomakomai	7·4	6	27
Quercus crispula	*Qc*	Sapporo	4·4	3	7
Quercus robur	*Qr*	Kew	6·2	6	13
Salix sachalinensis	*Ss*	Sapporo	8·5	5·5	13
Sorbus commixta	*Sc*	Sapporo	3·9	3	Unknown
Ulmus minor var. *vulgaris*	*Um*	Kew	5·0	4	7

Dye injection technique

The dye injection technique followed the methodology described by Sano *et al.* (2005) with a few modifications. The procedure started with adjusting the size of two large plastic funnels according to the stem diameter of the tree selected. One funnel was attached around the stem base and the second funnel was placed approx. 1 m above the first one. A vinyl, water-resistant tape was used to fix the funnels in place and to act as a sealant against leakages. For trees with a rough bark surface, an additional sealant was applied at the base and along the side of the funnel to support the vinyl tape in acting against leakages. An aqueous solution of 0·5 % acid fuchsin was filtered through a 0·22 μm filter after being stirred for 30 min or longer (see Sano *et al.*, 2005 for detailed information on the dye selected). The solution was poured into the receptacle that was set near the base of the stem, and notches as injecting channels were made using a sharp chisel at one side or four points around the stem. After approx. 1–3 h, liquid nitrogen was placed into the upper receptacle. After 5–10 min, 2–3 stem disks, 2–3 cm thick, were cut off the frozen section of each stem and placed into a flask containing liquid nitrogen. The disks were then freeze-dried for dye stabilization in preparation for stereoscopic dissection microscopy and light microscopy (LM). For species that were studied at Hokkaido University, one stem disk per tree was stored in liquid nitrogen for cryo-scanning electron microscopy (SEM).

To observe the distribution of the dye by LM, small cubes (approx. 2 mm^3) were cut and immersed in *n*-butyl glycidyl ether overnight. They were replaced with an epoxy resin that contained triglycidyl ether of glycerol, methyl nadic anhydride, dodecenylsuccinic anhydride and tri (dimethylaminomethyl) phenol at a ratio of 45:30:24:1 (v/v/v/v). The resin was then polymerized at 60 °C for 72 h. Sections of 4–8 μm in thickness were cut from the embedded specimens on an ultramicrotome using a glass knife under dry conditions. The sections were picked up with fine forceps, mounted in Bioleit and observed by LM. Acid fuchsin is insoluble in all solutions that were used for both embedding procedures and slide preparations. Therefore, the distribution of acid fuchsin remained unchanged once it had been freeze-dried.

Cryo-SEM

In order to obtain additional evidence on the conductive nature of ITEs, cryo-SEM was performed on the 11 tree species studied at Hokkaido University (Table 1). This technique allows observation of water-filled cells using a freeze-planing technique (Sano *et al.*, 1995; Utsumi and Sano, 2007). Frozen samples were trimmed and planed on a sliding microtome with disposable steel blades in a low temperature room at −23 °C. Frozen water in the wood samples was kept in a stable condition because humidity was controlled so as to prevent etching. The wood samples were slightly etched, coated with platinum and carbon in a cryo-SEM system (JSM840a equipped with a CRU-7000; JEOL Co., Tokyo, Japan) and observed at 3–5 kV.

Field-emission scanning electron microscopy (FE-SEM)

Similar preparation for FE-SEM was applied to nine species that had not been studied in two previous reports (Sano and Jansen, 2006; Sano *et al.*, 2008). Split samples were fixed on aluminium stubs next to each other in order to allow observation of complementary images of fractured pit pairs. This method was found to be essential for observing perforated pit membranes accurately and for distinguishing perforated pit membranes from ruptured pit membranes due to preparation artefacts (Sano and Jansen, 2006). The samples were coated with gold/palladium using an Emitech K550 sputter coater (Emitech Ltd, Ashford, UK) or with platinum using a Jeol JEE-4X vacuum evaporator (Jeol, Tokyo, Japan). Observations were carried out with a Hitachi S-4700 (Hitachi High Technologies Corp., Tokyo, Japan) at an accelerating voltage of 2 kV at the Royal Botanic Gardens, Kew and with a JSM-6301F (Jeol, Tokyo, Japan) at 2·5 kV at Hokkaido University.

Macerations

Macerations were prepared according to Franklin (1945). Small xylem slivers (longitudinal, radial and tangential dimensions were 5, 1 and 1 mm, respectively) were cut from the outer part of stem discs and soaked in a solution of 6 % hydrogen peroxide and acetic acid (1:1) at 60 °C for 72 h. After washing and gently shaking in water, a small amount of maceration tissue was placed on a microscope slide, dispersed with tweezers, mounted in glycerine and observed under a light microscope.

Anatomical measurements

Identification of ITE types in transverse wood sections was not always straightforward. However, careful observation of transverse sections from dye-injected samples in combination with cryo-SEM and macerations allowed us to distinguish the conductive from non-conductive cell types. The combination of these techniques was especially helpful to recognize in macerations and longitudinal sections (FE-SEM) the cell types and pit membrane features that corresponded to the cell types identified in transverse sections.

After careful observation of the ITE types in each species, quantitative measurements for cell length, pit density and pit size were based on 25 measurements of randomly selected cells. The average lumen surface area of ITEs was determined using transverse sections obtained from cryo-SEM and dye injection, and was based on a minimum of 100 measurements. All measurements were conducted using ImageJ (Rasband, 1997–2004). The pit shape was determined by calculating the circularity index of pits (= horizontal pit diameter/longitudinal pit diameter). Accurate measurements were difficult or impossible for particular cells types in a few species. For instance, quantifying the pit density was impossible in living ITEs of *Acer pictum* subsp. *mono* because of the occurrence of densely packed cell contents. Similarly, we were unable to distinguish the conductive from non-conductive ITEs in macerations of *Ilex aquifolium*. Therefore, data on cell length and mean number of pits for conductive and non-conductive cells were similar for this species (Table 3; Fig. 4C). We were also unable to measure the ITE lumen surface area for *I. aquifolium*, *Betula japonica*, and the living fibres in *Acer pseudoplatanus*.

The vessel grouping index was defined as the ratio of total number of vessels to the total number of vessel groupings (Carlquist, 1984). In addition, the solitary vessel index (ratio of the total number of solitary vessels to the total vessel grouping) and vessel multiple fraction (ratio of the grouped vessels to the total number of vessels) were calculated after quantifying the total number of vessels, solitary vessels, grouped vessels and vessel groupings for a minimum of 100 vessels (Jansen *et al.*, 2011). Both solitary vessels and grouped vessels (i.e. vessel multiples) were counted as a vessel group. Species with ring-porous woods, including *Fraxinus*, *Kalopanax*, *Quercus* and *Ulmus*, were excluded from the vessel grouping analyses because of large differences in spatial vessel distribution between earlywood and latewood.

Data analysis

Differences between conductive and non-conductive cells were analysed with independent samples *t*-tests. Linear regression analyses were used to determine the relationship between anatomical features. Statistical analyses were performed using the R statistical environment (R Development Core Team, 2008).

Wood anatomical terminology

Tracheary cell types that did not show a perforation plate as defined in the Introduction were described as ITEs. Since the presence of perforation plates, pit dimensions and other structural features could not be seen on transverse sections, maceration slides and longitudinal sections were used to distinguish cell types. Classification of cells types into fibre-tracheids, libriform fibres, true tracheids, vasicentric tracheids and vascular tracheids was avoided in the Results section.

The term 'perforated pit membrane' was used in relation to pit membrane characteristics of ITEs and should not be confused with true perforation plates of tracheary elements. Similarly to Sano and Jansen (2006), ITEs with perforated pit membranes were defined as having punctured or pierced pit membranes.

RESULTS

Dye injection experiments (Fig. 1)

There was a large interspecific variation in the dye distribution across growth rings. The frequency of stained (water-filled) vessels and the occurrence of conductive ITEs are summarized in Table 2. Detailed observations on ITEs are given Table 3.

In *A. pictum* subsp. *mono*, *A. pseudoplatanus*, *Framinus mandshurica* var. *japonica*, *Juglans mandshurica* var. *sieboldiana*, *Kalopanax septemlobus*, *Salix sachalinensis* and *Ulmus minor* var. *vulgaris*, the dye was limited to vessels (Fig. 1A–D). While the dye solution was occasionally found to stain axial and ray parenchyma cells that were in contact with vessels, no staining was detectable in ITEs in these seven species (Fig. 1C). In *B. japonica*, *I. aquifolium*, *Prunus sargentii*, *Quercus crispula* and *Quercus robur* the dye uptake stained not only cell walls of vessels, but also some of the ITEs (Fig. 1E–G). In these five species, the distributional pattern of the dye uptake in ITEs varied among species. In *B. japonica*, staining was rarely found in a few ITEs that made contact with vessels (Fig. 1E, arrow). In *I. aquifolium* and *P. sargentii*, the dye uptake was observed in cells distributed around vessels, although this tendency was not absolute (Fig. 1F). In the two *Quercus* species, the dye was consistently present in ITEs surrounding vessels, but absent from cells that were located away from vessels (Fig. 1G). In *Cercidiphyllum japonicum*, *Fagus crenata* and *Sorbus commixta*, the dye was found in almost all of the vessels and ITEs (Fig. 1H, I).

Cryo-SEM (Fig. 2)

In general, the results obtained by the dye injection method were similar to those of cryo-SEM. In *A. pictum* subsp. *mono*, *F. mandshurica* var. *japonica*, *J. mandshurica* var. *sieboldiana*, *K. septemlobus*, and *S. sachalinensis* almost all ITEs represented dead cells, indicating loss of cytoplasm and water in their cell lumina at or soon after their maturation (Fig. 2A, B). In the mature xylem of these species, most lumina of ITEs were completely empty, although living ITEs containing cytoplasm and dead elements with water-filled cell lumina were occasionally seen in some species (Fig. 2C, D). In *B. japonica*, water was rarely found in a few ITEs contacting vessels (Fig. 2E). The distributional pattern of water in *P. sargentii* and *Q. crispula* also resembled that of the dye uptake. In *P. sargentii*, ITEs that were filled with water tended to accumulate near vessels (Fig. 2F). In *Q. crispula*, water was only present in ITEs associated with vessels (Fig. 2G). In *C. japonicum*, *F. crenata* and *S. commixta*, almost all ITEs retained water in their lumina (Fig. 2H, I).

Pit membrane morphology (Fig. 3)

In *A. pictum* subsp. *mono*, *A. pseudoplatanus*, *K. septemlobus*, *F. mandshurica* var. *japonica*, *J. mandshurica* var. *sieboldiana*, *S. sachalinensis* and *U. minor* var. *vulgaris*, perforations of up to 2 μm in diameter were commonly present in pit membranes between the dead ITEs (Fig. 3A–D), while no such openings were detectable in pit membranes between living elements and between septate cells. The frequency of the perforated pit membranes between ITEs differed among taxa: from approx. 50 % in *K. septemlobus* and *U. minor* var. *vulgaris* to >80 % in the other species. In these seven species, no apparent pit pairs could be seen between vessel elements and ITEs using FE-SEM and LM (Table 3).

In *P. sargentii* and *I. aquifolium* both homogeneous (i.e. sheet-like) and perforated pit membranes were found between ITEs (Fig. 3E–H). The homogeneous pit membranes tended to appear between ITEs that were located near vessels (Fig. 3G). The homogeneous pit membranes of *P. sargentii* showed pseudo-tori as described by Jansen *et al.* (2007) (Fig. 3E, F). In perforated pit membranes of *I. aquifolium*, large, circular perforations tended to be eccentrically located (Fig. 3H). In *Q. robur*, pit membranes between ITEs surrounding vessels were always homogeneous (Fig. 3I), with pit membrane pores up to 300 nm frequently present near the periphery of the pit membrane. Pit membranes between other ITEs were

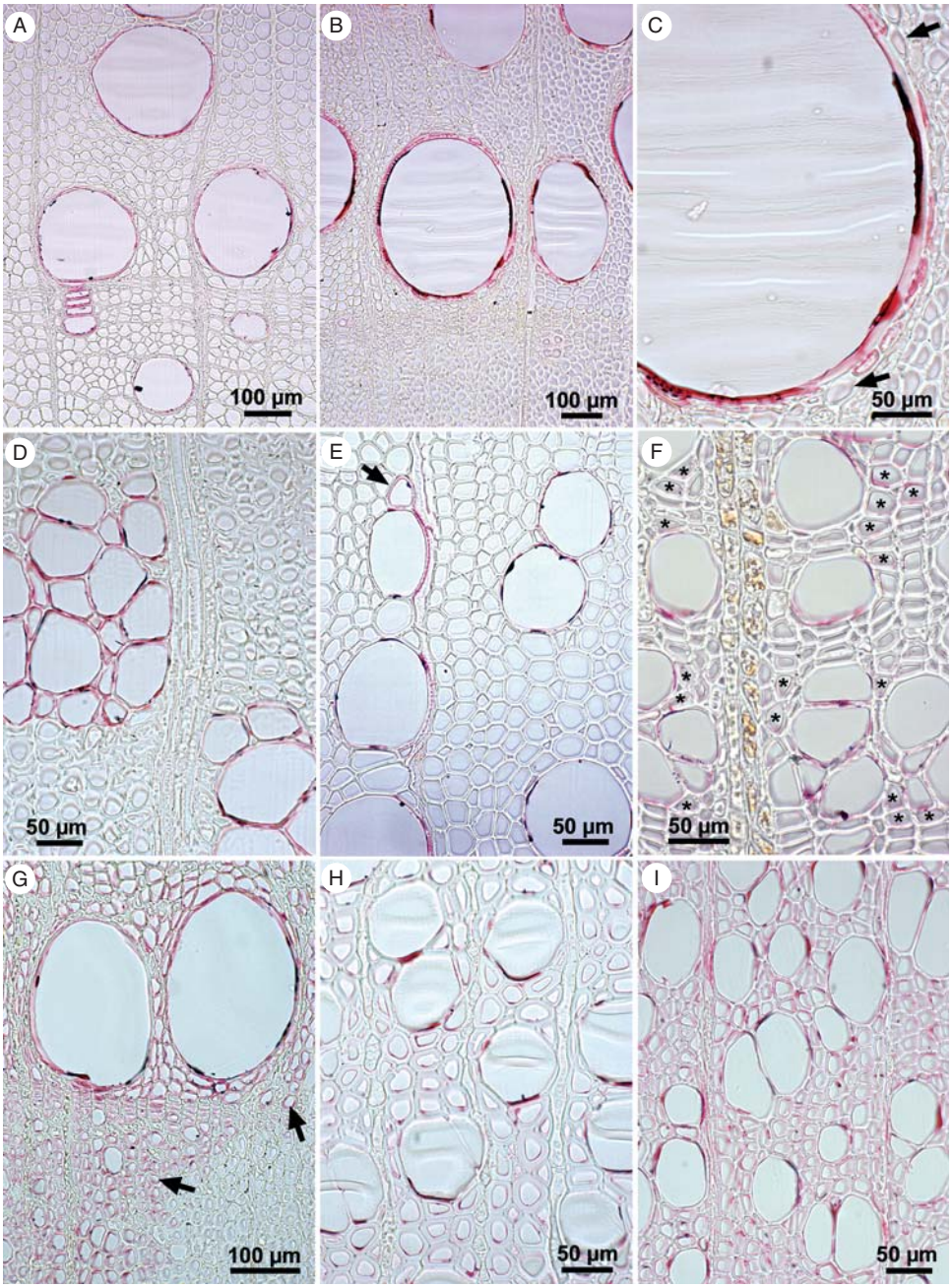

FIG. 1. LM images of transverse sections from angiosperm trees injected with a red dye (acid fuchsin); stems were shock-frozen and freeze-dried before sectioning; red cell walls specify cells that transport water. (A) *Juglans mandshurica* var. *sieboldiana* and (B) *Fraxinus mandshurica* var. *japonica*: water transport limited to vessels, earlywood from the outermost growth ring to latewood of the previous growth ring. (C) *Fraxinus mandshurica* var. *japonica*: detail of B; arrows indicate non-conductive imperforate tracheary elements (ITEs) that are in contact with a vessel. (D) Latewood of the outermost growth ring in *Kalopanax septemlobus* with non-conductive ITEs. (E) Central xylem area in a 1-year-old annual ring of *Betula japonica*. The arrow shows an ITE that is stained; all other ITEs are non-conductive. (F) *Prunus sargentii*: outer sapwood showing conductive vessels; both conductive (indicated by asterisks) and non-conductive ITEs occur. (G) *Quercus crispula*: earlywood of the current year's growth ring and latewood from the previous growth ring; conductive ITEs can be seen surrounding the two vessels and at the bottom left (indicated by arrows), while non-conductive ITEs mainly occur in the bottom right area. (H) *Cercidiphyllum japonicum* and (I) *Sorbus commixta*: earlywood of current year's growth ring; all imperforate cells are conductive.

commonly perforated in *Q. robur*. Also, pit pairs were present between vessel elements and adjacent ITEs.

In *C. japonicum* and *F. crenata* homogeneous pit membranes were always present between ITEs, with maximum pit membrane pores of 200 and 600 nm, respectively. These pit membrane pores were frequently found near the pit membrane annulus in >50 % of the pit membranes (Fig. 3J). In *S. commixta*, pseudo-tori with plasmodesmata remnants (visible as minute openings in Fig. 3K) were consistently associated with homogeneous pit membranes between ITEs, but no pit membrane pores were detected (Fig. 3K). In all three species, pit pairs were present between vessel elements and ITEs.

TABLE 2. *Vessel porosity (R, ring-porous; D, diffuse-porous) and the frequency of water-filled vessels as observed by cryo-SEM and dye injection in 15 angiosperm species*

Growth ring		*Am* D	*Ap* D	*Bj* D	*Cj* D	*Fc* D	*Fm* R	*Ia* D	*Jm* D	*Ks* R	*Ps* D	*Qc* R	*Qr* R	*Ss* D	*Sc* D	*Um* R
Current year	LW	a	–	a	c*	b*	a	–	a	a	a*	a*	–	a	a*	a*
	EW	b	a	a	a*	a*	a	c*	a	a	a*	a*	a*	a	a*	c
Second	LW	b	a	a	c*	c*	a	a*	a	a	a*	a*	a*	a	b*	a*
	EW	b	a	a	a*	a*	c	c*	b	c	a*	c*	a*	a	a*	c
Third	LW	b	c	a	–	c*	a	a*	b	a	a*	a*	a*	a	b*	a*
	EW	–	c	a	–	a*	–	c*	c	–	a*	–	a*	c	a*	c
Fourth	LW	–	–	a	–	–	–	b*	c	–	a*	–	a*	c	–	a*
	EW	–	–	a	–	–	–	c*	–	–	a*	–	a*	–	–	c
Fifth	LW	–	–	a	–	–	–	b*	–	–	b*	–	a*	–	–	c*
	EW	–	–	–	–	–	–	c*	–	–	b*	–	a*	–	–	c

Abbreviations correspond to the species listed in Table 1. Growth rings were counted from the bark towards the pith, with the current year's growth ring corresponding to the first ring. No latewood was formed in the current year's growth ring of *Ilex aquifolium* (Ia) and *Quercus robur* (Qr). One sample per species was studied. LW, latewood; EW, earlywood; a, water-filled vessels >70 %; b, water-filled vessels between 30 and 70 %; c, water-filled vessels <30 %; –, not examined. An asterisk indicates that conductive ITEs are present.

Quantitative analysis of pit and cell dimensions

The mean horizontal and longitudinal pit size (± s.d.) between ITEs was significantly smaller in non-conductive cells (5·09 ± 1 and 5·33 ± 0·5 μm, respectively) than in conductive elements (2·48 ± 0·9 and 2·78 ± 1 μm, respectively) (*t*-test; $P < 0·001$). There was also a significant difference between pit density of conductive and non-conductive cells (*t*-test; $t = 3·8329$, d.f. = 6·702, $P = 0·0069$), with an average number of 77 ± 35 (s.d.) pits in conductive cells and 24 ± 11 (s.d.) in non-conductive cells. No significant correlation (*t*-test; $t = 1·3744$, d.f. = 8·858, $P = 0·2031$) was noticed in pit shape, although conductive cells showed more circular pits (mean circularity index 0·95 ± 0·1) than non-conductive cells (mean circularity index 0·89 ± 0·06). Also, no correlation was found between the conductive function and cell length of ITEs (Table 3). In general, pits in conductive cells were common in both radial and tangential walls, while non-conductive cells only showed pits associated with radial walls. However, exceptions to this pattern were found in *A. pictum* subsp. *mono*, *I. aquifolium*, *P. sargentii*, *Q. crispula* and *Q. robur* (Table 3). All septate ITEs were non-conductive.

There was a linear correlation between the pit diameter and pit density (Pearson correlation, $r = 0·85$ for horizontal pit diameter, $r = 0·79$ for longitudinal pit diameter, $P < 0·0001$; Fig. 4A). The pit shape was negatively correlated with cell length ($r = –0·53$, $P = 0·0188$), but positively associated with pit density ($r = 0·63$, $P = 0·0035$), suggesting that circular pits occurred in relatively short ITEs with a high number of pits, while more elliptical pits were observed in long ITEs with a low number of pits. Conductive ITEs were larger in lumen surface area than non-conductive ITEs (Table 3), but this correlation seemed only valid within a single species with both conductive and non-conductive ITEs and not across all 15 species studied. There was no significant correlation between cell length and pit diameter, and between cell length and pit density (Fig. 4B, C). Quantitative vessel grouping characteristics such as vessel grouping index, solitary vessel index and vessel multiple fraction (data not shown) showed no correlation with anatomical features of ITEs in the species with diffuse-porous wood.

DISCUSSION

The observations demonstrate that water transport through ITEs can be either present or absent. This functional difference usually goes hand in hand with morphological characteristics of ITEs and their spatial distribution within the hydraulic network of vessel bearing plants. It is generally thought that narrow ITEs carry an insignificant amount of water compared with vessels, which are much wider and hydraulically more efficient. Assuming that average vessel diameters are ten times larger than conductive ITEs, this would mean that vessels conduct 10 000 times more water than ITEs because the flow rate of water through a conductive cell is proportional to the fourth power of the cell's diameter (Tyree and Zimmermann, 2002).

However, based on the observed variation in vessel conductivity across growth rings, ITEs could play an important role as a back-up or auxiliary transport system when vessels become embolized and no longer refill. With respect to the distribution of water-filled vessels (Table 2), most species appear to show higher amounts of cavitation in earlywood than in latewood, but in *F. crenata*, *S. commixta* and *C. japonicum* the opposite is found (i.e. more embolism in latewood than in earlywood). Although conductive ITEs are found in species belonging to both groups, vessels were reported to be more embolized than conductive ITEs. This is especially clear in species with ring porosity in which the majority of large earlywood vessels remain functional for only one season, while almost all of the latewood ITEs were found to be functional up to nine growth rings in *U. minor* var. *vulgaris*. These observations are in line with earlier reports for *Ulmus americana* (Ellmore and Ewers, 1985, 1986). With respect to *Ulmus*, these observations should also be linked with the occurrence of torus-bearing pit membranes that are restricted to ITEs and absent in vessel pits (Jansen *et al.*, 2004). Since conduits with large diameters generally embolize more easily than

TABLE 3. *Selected data of qualitative and quantitative features (± s.d.) associated with imperforate tracheary elements (ITEs). The order of the species is based on the conductive or non-conductive nature of the ITEs as determined by dye-injection experiments and cryo-SEM*

Species	Function	Pit membrane type between ITEs	Pits between vessels and ITEs	Pits on tangential wall	Mean ITE length (mm)	Mean number of pits per ITE	Mean horizontal pit diameter (μm)	Mean longitudinal pit diameter (μm)	Pit shape	ITE lumen surface area (μm^2)
Cj	C	Sheet-like	Pit pair	Common	1·62 ± 0·19	81 ± 32·8	4·8 ± 0·45	5·4 ± 0·75	0·89 ± 0·15	62·7 ± 30·9
Fc	C	Sheet-like	Pit pair	Common	1·16 ± 0·15	56 ± 31·7	4·3 ± 0·42	5 ± 0·5	0·86 ± 0·12	40·4 ± 24·5
Ia	C	Sheet-like	Pit pair	Common	1·26 ± 0·23	47·16 ± 23·09	5·5 ± 0·52	5·9 ± 0·41	0·93 ± 0·11	–
Ps	C	Sheet-like	Pit pair	Common	0·51 ± 0·09	66 ± 31	4·3 ± 0·67	4·6 ± 0·46	0·93 ± 0·17	37·9 ± 19·2
Qc	C	Sheet-like	Pit pair	Common	0·64 ± 0·14	139 ± 33·8	6 ± 0·47	5·9 ± 0·57	1·02 ± 0·13	82·92 ± 30·8
Qr	C	Sheet-like	Pit pair	Common	0·73 ± 0·11	112·4 ± 29·54	6·7 ± 1·66	5·9 ± 0·52	1·14 ± 0·3	143·5 ± 52·1
Sc	C	Sheet-like	Pit pair	Common	1·01 ± 0·11	43 ± 12·7	4 ± 0·21	4·6 ± 0·37	0·87 ± 0·08	28·2 ± 10·5
Um	C	–	Pit pair	Common	0·28 ± 0·05	–	–	–	–	234·7 ± 150
Am	NC	Perforated	No pits	Common	0·61 ± 0·08	17 ± 7·7	1·9 ± 0·49	2·1 ± 0·56	0·90 ± 0·34	46·1 ± 24·7
Am	NC	–	No pits	Rare	0·4 ± 0·08	–	–	–	–	82·3 ± 18·3
Ap	NC	Perforated	No pits	Rare	0·54 ± 0·06	21·6 ± 8·32	2 ± 0·69	2·2 ± 0·61	0·91 ± 0·4	147·9 ± 55
Ap	NC	–	No pits	Rare	–	–	–	–	–	–
Bj	NC*	Perforated	Blind pits	Rare	1·12 ± 0·2	44 ± 15·2	2·9 ± 0·43	3·4 ± 0·59	0·85 ± 0·19	–
Fm	NC	Perforated	No pits	Rare	0·91 ± 0·16	32 ± 11·7	2·1 ± 0·57	2·4 ± 0·56	0·88 ± 0·31	38·3 ± 34·4
Ia	NC	Perforated	No pits	Common	1·26 ± 0·23	47·16 ± 23·09	4·5 ± 0·5	4·9 ± 0·49	0·92 ± 0·14	–
Jm	NC	Perforated	No pits	Rare	1·08 ± 0·17	27 ± 16·8	3·3 ± 0·68	3·6 ± 0·73	0·92 ± 0·27	105·1 ± 90·2
Ks	NC	Perforated	No pits	Rare	0·87 ± 0·13	26 ± 7·9	1·6 ± 0·48	1·6 ± 0·36	1·00 ± 0·38	54·8 ± 28·69
Ks	NC	–	No pits	Rare	0·8 ± 0·11	27 ± 6·5	–	–	–	66·88 ± 29·8
Ps	NC	Perforated	No pits	Common	1·05 ± 0·31	23 ± 6·3	3·7 ± 0·79	4·1 ± 0·73	0·90 ± 0·25	29·54 ± 17·6
Qc	NC	Perforated	No pits	Common	1·16 ± 0·14	12 ± 4·7	2·2 ± 0·4	2·5 ± 0·36	0·88 ± 0·2	26·45 ± 20·9
Qr	NC	Perforated	No pits	Common	1·17 ± 0·19	10·71 ± 6·51	2·6 ± 0·28	3 ± 0·31	0·87 ± 0·13	67·4 ± 29·5
Ss	NC	Perforated	Blind pits	Rare	0·94 ± 0·16	21 ± 7·8	1·5 ± 0·37	1·6 ± 0·31	0·94 ± 0·29	39·53 ± 29·7
Um	NC	Perforated	No pits	Rare	1·47 ± 0·18	8·16 ± 3·83	1·4 ± 0·22	1·9 ± 0·26	0·74 ± 0·15	42·68 ± 17·6

Abbreviations correspond to the species listed in Table 1. Both conductive and non-conductive ITEs were found in five out of 15 angiosperm species. Conductive ITEs could not be distinguished from non-conductive ones in macerations slides of *Ilex aquifolium* (*Ia*), resulting in similar values for mean ITE length and number of pits per cell. –, unknown; *, conductive ITEs were rarely found in *Betula japonica* (*Bj*); C, conductive; NC, non-conductive.

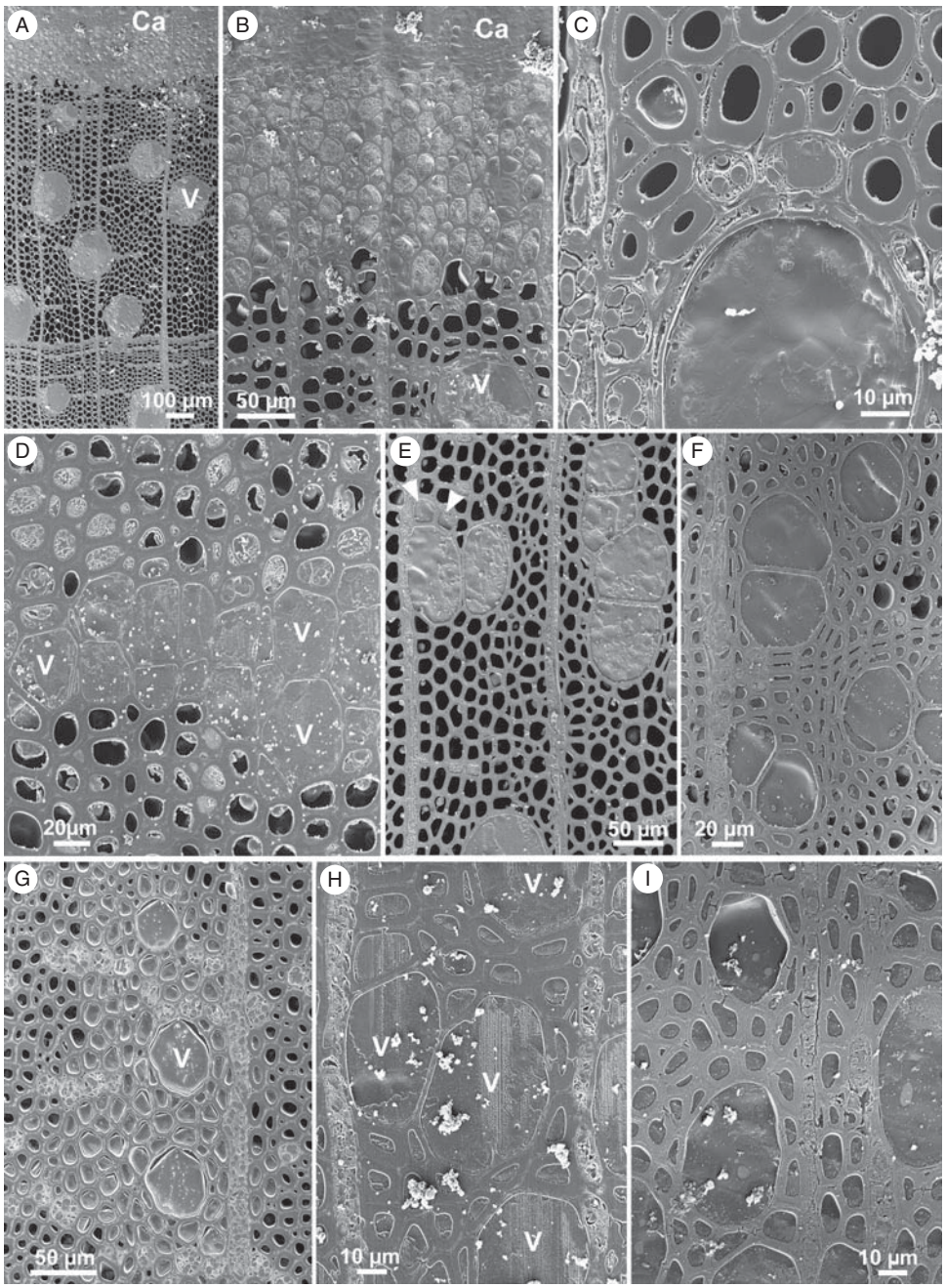

FIG. 2. Cryo-scanning electron micrographs of dye-injected trees; after shock-freezing, transverse surfaces were trimmed using a freeze-planing technique; this method allows water-filled cells to be distinguished from embolized or non-conductive cells. (A and B) *Juglans mandshurica* var. *sieboldiana*: water-filled vessels (V) and developing xylem elements near cambium (Ca). (C) *Fraxinus mandshurica* var. *japonica*: a water-filled vessel and non-conductive tracheary elements from the outermost growth ring. (D) Latewood of the outermost growth ring of *Kalopanax septemlobus* showing water-filled vessels (V), living imperforate tracheary elements (ITEs) containing cytoplasm, and elements with water-filled lumina. (E) Central xylem area in a 1-year-old annual ring of *Betula japonica*. The arrows point to two ITEs that are conductive. (F) Outer sapwood of *Prunus sargentii* showing ITEs filled with water surrounding vessels. (G) Narrow latewood vessels (V) from the current's year growth ring in *Quercus crispula*; conductive ITEs surrounding vessels. (H and I) Inner layer of the outermost growth ring of *Cercidiphyllum japonicum* (H) and *Sorbus commixta* (I) demonstrating that all vessels and ITEs are water filled.

narrow conduits as a consequence of frost- and/or drought-induced cavitation (Davis *et al.*, 1999; Cai and Tyree, 2010; Pittermann, 2010), conductive ITEs can be suggested to be more cavitation resistant than vessels. Further experimental work combining cavitation experiments with dye injection and cryo-SEM would be most useful to test current ideas about the functional 'longevity' of vessels and tracheids and whether any difference in their refilling capacity may occur.

Overall, the data obtained are in general agreement with earlier studies, as similar staining patterns were previously obtained for *Acer*, *Kalopanax*, *Prunus*, *Quercus*, *Salix* and *Ulmus* (Ellmore and Ewers, 1985, 1986; Umebayashi *et al.*,

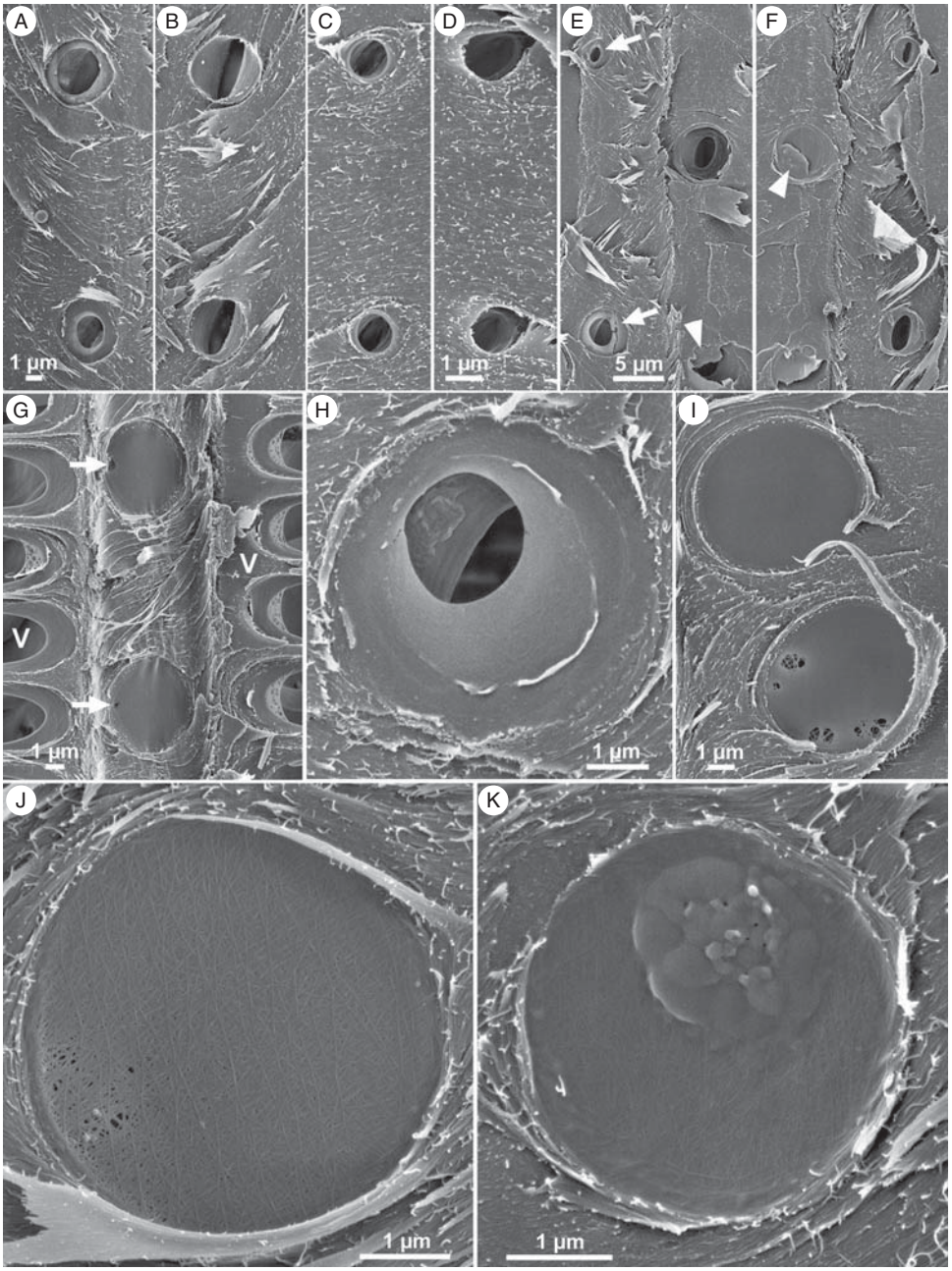

FIG. 3. Scanning electron micrographs of pits between imperforate tracheary elements (ITEs). (A–D) A complementary image of fractured pit pairs between ITEs with perforated pit membranes in *Juglans mandshurica* var. *sieboldiana* (A, B) and *Ulmus minor* var. *vulgaris* (C, D). (E and F) A complementary image of four fractured pit pairs between ITEs showing two pairs with perforated pit membranes (arrows) and two pit pairs with pseudo-tori (arrowheads) in *Prunus sargentii*. (G) Homogeneous pit membranes in an ITE sandwiched by two vessels (V) in *Ilex aquifolium*. Arrows indicate pit membrane pores. (H) A perforated pit membrane in an ITE of *Ilex aquifolium*. (I) and (J) Homogeneous pit membranes in an ITE of *Quercus robur* (I) and *Cercidiphyllum japonicum* (J) showing relatively large pit membranes pores. (K) A homogeneous pit membrane with a pseudo-torus in an ITE of *Sorbus commixta*.

2008, 2010). Our cryo-SEM observations fully support the results obtained by dye injection, confirming the valid approach of both techniques. The only exception noticed by us was the occasional observation under cryo-SEM of water-filled cells surrounding vessels in *F. mandshurica* var. *japonica* (Fig. 2C), while similar cells were not stained using the dye technique. Umebayashi *et al.* (2008, 2010) demonstrated similar findings in *Acer palmatum*, *Salix gracilistyla* and *Dendropanax trifidus*, but the opposite situation (i.e. dye uptake but no observation of water under cryo-SEM) has not been reported as far as we know. It is possible that the transport efficiency of narrow ITEs is very low and that more time is required during dye injection experiments before the dye penetrates all conductive ITEs.

Interestingly, our morphological observations provide evidence that the pit membrane structure of ITEs is closely correlated with their conductive nature: homogeneous pit membranes are associated with pit pairs between conductive

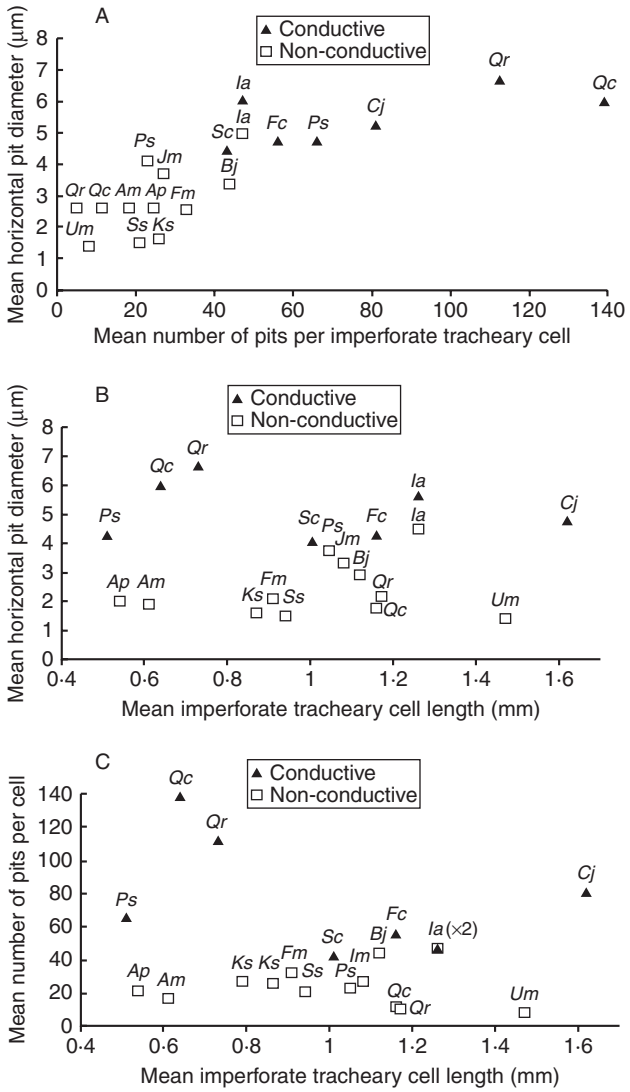

FIG. 4. Relationship between anatomical features of imperforate tracheary elements (ITEs) with reference to their conductive vs. non-conductive nature for 15 species. Abbreviations correspond to those given Table 1. All data represent average values based on 25 measurements from one sample per species. (A) Relationship between horizontal pit diameter and pit number per cell. (B) Relationship between cell length and horizontal pit diameter (C) Relationship between cell length and pit number per cell. Conductive and non-conductive cells could not be distinguished in maceration slides of *Ilex aquifolium* (Ia), resulting in similar values for this species.

ITEs, while perforated pit membranes were characteristic of non-conductive cells. These findings support earlier evidence on the distribution of perforated pit membranes (Sano and Jansen, 2006), indicating that the homogeneous vs. perforated pit membranes represent a useful, although practically difficult character for distinguishing conductive from non-conductive cells. While sample preparation (splitting and scraping in combination with alcohol treatment, dehydration and coating) may result in artefacts of pit membrane pores (Jansen *et al.*, 2008, 2009), artificial pores can usually be distinguished from true pores by carefully observing where cell walls have been split and which parts are left intact in complementary samples of fractured pit pairs. Therefore, we feel confident that the FE-SEM observations of non-conductive ITEs with perforated pit membranes do not represent artefacts.

Cryo-SEM showed that ITEs with perforated pit membranes between their cells become dehydrated at or soon after maturation, while cells with homogeneous, sheet-like pit membranes retain water after maturation. How exactly these perforated pit membranes are formed is unknown. Since the pit membrane perforations (up to 2 μm in diameter) are larger than pit membranes pores (up to 600 nm in *F. crenata*), the occurrence of perforated pit membranes appears to be an important feature in suppressing the conductive function of ITEs. While maximum pit membrane pore sizes are usually <100 nm, large pores have previously been observed in intervessel pit membranes (Choat *et al.*, 2004, 2008; Sano, 2005).

Moreover, pit pairs are present between a vessel and a functional ITE, but no pits or only blind pits are found between a vessel and a non-conductive ITE. It is possible that the absence of pit pairs between a vessel and non-conductive ITEs with perforated pit membranes contributes to the safety of the conductive cells. If functional vessels would be connected to non-conductive ITEs by pit pairs, this could result in a weakening of the cell wall and a high chance for air-seeding through the vessel–ITE pits. In other words, vessel-bearing species with non-conductive ITEs avoid cavitation risks by not forming pit connections from a functioning vessel to non-conductive ITEs with perforated pit membranes.

The major morphological features associated with the conductivity of tracheary elements include the pit size, pit density and pit distribution, which have repeatedly been used as criteria to distinguish different types of ITEs (Baas, 1986; Carlquist, 1986*a*, *b*, 2001; Rosell *et al.*, 2007). A large pit size and high pit density in combination with pit distribution on both tangential and radial walls are thought to be useful features for efficient water conduction. Therefore, it is not surprising that large pit borders and high pit density are significantly higher in conductive elements than in non-conductive elements. It is possible that conductive ITEs sacrifice to some extent the mechanical support function for water conduction by securing a larger wall area for pits (Carlquist, 2001). Since pit occurrence on tangential and radial walls is not always strictly associated with water transport in ITEs, it is recommended to use this feature in combination with other pit characteristics. Furthermore, our data do not provide evidence that the cell length is related to water transport as could be expected according to the Baileyan trends (Bailey and Tupper, 1918; Metcalfe and Chalk, 1983; Carlquist, 2001). It is possible that the low number of species studied herein does not support this trend. Alternatively, due to variation in tree age between the species studied, which varied from 4 to >20 years, it is possible that the length of ITEs is influenced by age-related variation within a single tree (Panshin and De Zeeuw, 1980; Metcalfe and Chalk, 1983).

The present results do not show any relationship between conductivity of ITEs and vessel grouping in the ten species studied with diffuse-porous wood. Nevertheless, the nature of ITEs has been demonstrated to be closely linked with the spatial distribution of vessels: species that possess solitary vessels frequently show tracheids *sensu* Carlquist, whereas

libriform fibres and fibre-tracheids are more common if vessels are grouped to a lesser or greater extent (Carlquist, 1984, 2009*b*; Carlquist and Hoekman, 1985; Rosell *et al.*, 2007; Wheeler *et al.*, 2007). Including a higher number of species and/or species with a large variation in vessel grouping would be recommended to test this hypothesis.

Confusion regarding the conductive or non-conductive nature of fibre-tracheids is largely a terminological issue. Based on the physiological data presented herein, we propose defining all functional ITEs as tracheids, while non-conductive ITEs represent either fibre-tracheids or libriform fibres. With respect to the species studied herein, this implies that tracheids occur in *F. crenata*, *P. sargentii*, *C. japonica*, *I. aquifolium* and *S. commixta*, in addition to vascular tracheids in *U. minor* var. *vulgaris* and vasicentric tracheids in *Q. crispula* and *Q. robur*. While only one type of conductive ITEs occurs in *Fagus*, *Cercidiphyllum* and *Sorbus*, there are both conductive and non-conductive ITEs in *P. sargentii* and *I. aquifolium*, which are considered as tracheids and fibre-tracheids, respectively. Given the differences in pit dimensions between the conductive and non-conductive cells in *P. sargentii* and *I. aquifolium*, there is morphological evidence for supporting this terminology. In addition to the concept of Metcalfe and Chalk (1950), who defined tracheids as 'fibres with fully bordered pits', we suggest that tracheids should show non-perforated intertracheid pit membranes as well as tracheid–vessel pit pairs. In this way, we support Carlquist's (1985, 2001, 2009*b*) broader definition of tracheids because of the following two reasons: (1) identifying all conductive ITEs as a single ITE type (tracheid) is more meaningful from a functional point of view than having more than one conductive ITE type; and (2) the correlation between spatial vessel distribution and ITE types (Carlquist 1966, 1984, 1987, 2001, 2009*b*; Rosell *et al.*, 2007), although statistically not supported by the data herein, is most significant when applying a broad tracheid definition. Nevertheless, this report is only a first step in opening links between the anatomy and physiological role of ITEs, and is certainly not comprehensive. More work on carefully selected species showing diverse wood anatomical patterns would be most welcome to provide additional evidence.

Based on observations within the genus *Acer*, Vazquez-Cooz and Meyer (2006, 2008) suggested that the presence of intercellular spaces and histochemistry of secondary cell walls may offer additional criteria to distinguish libriform fibres from fibre-tracheids. More research is certainly needed on developmental and histochemical aspects of ITEs. Since the narrow lumen size in ITEs does not favour visualization of water transport *in vivo* using non-invasive imaging techniques such as magnetic resonance imaging and X-ray computed tomography (Holbrook *et al.*, 2001; Kaufmann *et al.*, 2009), we suggest that further understanding of the conductive nature of ITEs could greatly benefit from detailed anatomical observations in combination with experiments such as dye injection and/or cryo-SEM. Given the morphological differences between ITEs, we believe that special attention to anatomical features such as pit membranes provides a suitable way to understand further the functional significance of hydraulic conductivity in ITEs.

ACKNOWLEDGEMENTS

Ms A. Pletsers and Mrs A. Lynch (RBG, Kew) are acknowledged for assistance with dye injection experiments. We are grateful to Mr T. Kirkham (RBG, Kew) for permission to apply the dye experiment to trees from the living collections of Kew. The 'A year at Kew series 3′ film crew is acknowledged for helping us with presenting our project to a wide audience. We thank Dr T. Shiraiwa, Dr S. Matoba and Mr S. Kanamori for permission to use the special low-temperature room at the Institute of Low Temperature Sciences (Hokkaido University, Japan). We also thank Dr F. Lens (K.U.Leuven, Belgium) and two reviewers for useful comments on an earlier version of this manuscript. This work was supported by a Grant-in-Aid for Scientific Research from JSPS, Japan (grant numbers 18580158, 20580171) to Y.S. and the Ministry of Science, Research, and the Arts (Baden-Wurttemberg, Germany) to S.J.

LITERATURE CITED

Baas P. 1986. Terminology of imperforate tracheary elements – in defense of libriform fibres with minutely bordered pits. *International Association of Wood Anatomists Bulletin* **7**: 82–86.

Baas P, Magendans JFC. 1999. Review and debate: hardwood fibre pits – again! *International Association of Wood Anatomists Journal* **20**: 456–459.

Bailey IW, Tupper WW. 1918. Size variation in tracheary cells: I. A comparison between the secondary xylems of vascular cryptograms, gymnosperms, and angiosperms. *Proceedings of the American Academy of Arts and Sciences* **54**: 149–204.

Bailey IW. 1936. The problem of differentiating and classifying tracheids, fiber-tracheids and libriform fibers. *Tropical Woods* **45**: 18–23.

Braun HJ. 1970. Funkionelle Histologie der sekundären Sprossachse. In: Zimmermann W, Ozenda P, Wulff HD, eds. *Encyclopedia of plant physiology*, 2nd edn. Berlin: Gebrüder Borntraeger, 1–190.

Butterfield BG, Meylan BA 1976. The occurrence of septate fibres in some New Zealand woods. *New Zealand Journal of Botany* **14**: 123–130.

Butterfield BG. 1995. Vessel element differentiation. In: Iqbal M, ed. *The cambial derivatives.* Berlin: Gebrüder Borntraeger, 93–106.

Cai J, Tyree MT. 2010. The impact of vessel size on vulnerability curves: data and models for within-species variability in saplings of aspen, *Populus tremuloides* Michx. *Plant, Cell and Environment* **33**: 1059–1069.

Carlquist S. 1966. Wood anatomy of Compositae: a summary, with comments on factors controlling wood anatomy. *Aliso* **6**: 25–44.

Carlquist S. 1984. Vessel grouping in dicotyledon wood: significance and relationship to imperforate tracheary elements. *Aliso* **10**: 505–525.

Carlquist S. 1985. Vasicentric tracheids as a drought surivival mechanism in the woody flora of southern California and similar regions; review of vasicentric tracheids. *Aliso* **11**: 37–68.

Carlquist S. 1986*a*. Terminology of imperforate tracheary elements. *International Association of Wood Anatomists Bulletin* **7**: 75–81.

Carlquist S. 1986*b*. Terminology of imperforate tracheary elements. A reply. *International Association of Wood Anatomists Bulletin* **7**: 168–170.

Carlquist S. 1987. Diagonal and tangential vessel aggregations in wood: function and relationship to vasicentric tracheids. *Aliso* **11**: 451–462.

Carlquist S. 2001. *Comparative wood anatomy: systematic, ecological, and evolutionary aspects of dicotyledon wood*, 2nd edn. Berlin: Springer-Verlag.

Carlquist S. 2009*a*. Xylem heterochrony: an unappreciated key to angiosperm origin and diversifications. *Botanical Journal of the Linnean Society* **161**: 26–65.

Carlquist S. 2009*b*. Non-random vessel distribution in woods: patterns, modes, diversity, correlations. *Aliso* **27**: 39–58.

Carlquist S, Hoekman DA. 1985. Ecological wood anatomy of the woody southern Californian flora. *International Association of Wood Anatomists Bulletin* **6**: 319–347.

Choat B, Jansen S, Zwieniecki MA, Smets E, Holbrook NM. 2004. Changes in pit membrane porosity due to deflection and stretching: the role of vestured pits. *Journal of Experimental Botany* **55**: 1569–1575.

Choat B, Cobb AR, Jansen S. 2008. Structure and function of bordered pits: new discoveries and impacts on whole-plant hydraulic function. *New Phytologist* **177**: 608–626.

Davis SD, Sperry JS, Hacke UG. 1999. The relationship between xylem conduit diameter and cavitation caused by freezing. *American Journal of Botany* **86**: 1367–1372.

Ellmore GS, Ewers FW. 1985. Hydraulic conductivity in trunk xylem of elm, *Ulmus americana*. *International Association of Wood Anatomists Bulletin* **6**: 303–307.

Ellmore GS, Ewers FW. 1986. Fluid flow in the outermost xylem increment of a ring-porous tree, *Ulmus americana*. *American Journal of Botany* **73**: 1771–1774.

Franklin GL. 1945. Preparation of thin sections of synthetic resins and wood–resin composites, and a new macerating method for wood. *Nature* **155**: 51.

Holbrook NM, Ahrens ET, Burns MJ, Zwieniecki MA. 2001. *In vivo* observation of cavitation and embolism repair using magnetic resonance imaging. *Plant Physiology* **126**: 27–31.

Hudson PJ, Razanatzoa J, Feild TS. 2010. Early vessel evolution and the diversification of wood function: insights from Malagasy Canellales. *American Journal of Botany* **97**: 80–93.

Jansen S, Lens F, Ntore S, Piesschaert F, Robbrecht E, Smets E. 2001. Contributions to the systematic wood anatomy of the Rubioideae (Rubiaceae). *Journal of Plant Research* **114**: 269–289.

Jansen S, Choat B, Vinckier S, Lens F, Schols P, Smets E. 2004. Intervascular pit membranes with a torus in the wood of *Ulmus* (Ulmaceae) and related genera. *New Phytologist* **163**: 51–59.

Jansen S, Sano Y, Choat B, Rabaey D, Lens F, Dute R. 2007. Pit membranes in tracheary elements of Rosaceae and related families. *American Journal of Botany* **94**: 503–514.

Jansen S, Pletsers A, Sano Y. 2008. The effect of preparation techniques on SEM-imaging of pit membranes. *International Association of Wood Anatomists Journal* **29**: 161–178.

Jansen S, Choat B, Pletsers A. 2009. Morphological variation of intervessel pit membranes and implications to xylem function in angiosperms. *American Journal of Botany* **96**: 409–419.

Jansen S, Gortan E, Lens F, *et al*. 2011. Do quantitative vessel and pit characters account for ion-mediated changes in the hydraulic conductance of angiosperm xylem? *New Phytologist* **189**: 218–228.

Kaufmann I, Schulze-Till T, Schneider HU, Zimmermann U, Jakob P, Wegner LH. 2009. Functional repair of embolized vessels in maize roots after temporal drought stress, as demonstrated by magnetic resonance imaging. *New Phytologist* **184**: 245–256.

Koek-Noorman J. 1969. A contribution to the wood anatomy of South American (chiefly Suriname) Rubiaceae I. *Acta Botanica Neerlandica* **18**: 108–123.

Lens F, Smets E, Gasson P, Jansen S. 2003. Comparative wood anatomy of epacrids (Styphelioideae, Ericaceae s.l.). *Annals of Botany* **91**: 835–856.

Lens F, Kårehed J, Baas P, *et al*. 2008. The wood anatomy of the polyphyletic Icacinaceae s.l. revisited within asterids. *Taxon* **57**: 525–552.

Lens F, Endress ME, Baas P, Jansen S, Smets E. 2009. Vessel grouping patterns in subfamilies Apocynoideae and Periplocoideae confirm phylogenetic value of wood structure within Apocynaceae. *American Journal of Botany* **96**: 2168–2183.

Magendans JFC. 1999. Morphology of pits in hardwood fibres. *Wageningen Agricultural University Papers* **99**: 1–100.

Metcalfe CR, Chalk L. 1950. *Anatomy of the dicotyledons*. Oxford: Clarendon Press.

Metcalfe CR, Chalk L. 1983. *Anatomy of the dicotyledons. Volume II. Wood structure and conclusions of the general introduction*, 2nd edn. Oxford: Clarendon Press.

Panshin AJ, De Zeeuw C. 1980. *Textbook of wood technology*. New York: McGraw-Hill.

Parameswaran N, Liese W. 1969. On the formation and fine structure of septate wood fibres of *Ribes sanguineum*. *Wood Science and Technology* **3**: 272–236.

Pittermann J. 2010. The evolution of water transport in plants: an integrated approach. *Geobiology* **8**: 112–139.

R Development Core Team. 2008. *R: A language and environment for statistical computing*. Vienna: R Foundation for Statistical Computing.

Rasband WS. 1997–2004**.** *ImageJ*. National Institutes of Health: http://rsb.info.nih.gov/ij/.

Reinders E. 1935. Fiber-tracheids, libriform wood fibers, and systematics in wood anatomy. *Tropical Woods* **44**: 30–36.

Reinders E. 1951. On the distinction between fiber-tracheids and libriform wood fibers. *International Association of Wood Anatomists Bulletin* **1951**: 2–6.

Rosell JA, Olson M, Aguirre-Hernández R, Carlquist S. 2007. Logistic regression in comparative wood anatomy: tracheid types, wood anatomical terminology, and new inferences from the Carlquist and Hoekman southern Californian data set. *Botanical Journal of the Linnean Society* **154**: 331–351.

Sano Y. 2005. Inter- and intraspecific structural variations among intervascular pit membranes as revealed by field-emission scanning electron microscopy. *American Journal of Botany* **92**: 1077–1084.

Sano Y, Jansen S. 2006. Perforated pit membranes of imperforate tracheary elements in some angiosperms. *Annals of Botany* **97**: 1045–1053.

Sano Y, Fujikawa S, Fukazawa K. 1995. Detection and features of wetwood in *Quercus mongolica* var. *grosseserrata*. *Trees* **9**: 261–268.

Sano Y, Okamura Y, Utsumi Y. 2005. Visualizing water-conducting pathways of living trees: selection of dyes and tissue preparation methods. *Tree Physiology* **25**: 269–275.

Sano Y, Ohta T, Jansen S. 2008. The distribution and structure of pits between vessels and imperforate tracheary elements in angiosperm woods. *International Journal of Wood Anatomists Journal* **29**: 1–15.

Sperry JS, Hacke UG, Field T, Sano Y, Sikkema EH. 2007. Hydraulic consequences of vessel evolution in angiosperms. *International Journal of Plant Science* **168**: 1127–1139.

Tyree MT, Zimmermann MH. 2002. *Xylem structure and the ascent of sap*, 2nd edn. New York: Springer-Verlag.

Umebayashi T, Utsumi Y, Koga S, *et al*. 2008. Conducting pathways in north temperate deciduous broadleaved trees. *International Journal of Wood Anatomists Journal* **29**: 247–263.

Umebayashi T, Utsumi Y, Koga S, *et al*. 2010. Xylem water-conducting patterns of 34 broadleaved evergreen trees in southern Japan. *Trees* **3**: 571–583.

Utsumi Y, Sano Y. 2007. Cryoplaning technique for visualizing the distribution of water in woody tissues by cryoscanning electron microscopy. In: Kuo J, ed. *Electron microscopy: methods and protocols*, 2nd edn. Totowa, NJ: Humana Press, 497–506.

Vazquez-Cooz I, Meyer RW. 2006. Distribution of libriform fibers and presence of spiral thickenings in fifteen species of Acer. *International Journal of Wood Anatomists Journal* **27**: 173–182.

Vazquez-Cooz I, Meyer RW. 2008. Fundamental differences between two fiber types in Acer. *International Journal of Wood Anatomists Journal* **29**: 129–141.

Wheeler EA, Baas P, Rodgers S. 2007. Variations in dicot wood anatomy – a global analysis based on the Inside Wood database. *International Journal of Wood Anatomists Journal* **28**: 229–258.